Comparison of Doxorubicin Concentration Profiles in Radiofrequency-Ablated Rat Livers from Sustained- and Dual-Release PLGA Millirods

Feng Qian,[1,4] Nicholas Stowe,[2] Gerald M. Saidel,[1] and Jinming Gao[1,3]

Received November 7, 2003; accepted November 18, 2003

Purpose. To evaluate and compare the local pharmacokinetics of doxorubicin in radiofrequency (rf)-ablated rat livers after interstitial delivery from sustained- and dual-release poly(D,L-lactide-*co*-glycolide) (PLGA) millirods.

Methods. PLGA millirods with sustained- and dual-release kinetics (burst followed by sustained release) of doxorubicin were implanted in rf-ablated rat livers. Doxorubicin release kinetics *in vivo* were measured from explanted millirods by UV-Vis spectrophotometer over 8 days. Spatial distribution of doxorubicin in liver tissues was measured by fluorescence imaging.

Results. In the initial 24 h after millirod implantation, dual-release millirods released significantly more doxorubicin into liver tissues than the sustained millirods. Subsequently, both types of millirods provided comparable sustained-release kinetics over 8 days. With dual-release millirods, doxorubicin concentration and penetration distance in liver tissue increased more rapidly. To reach 30 μg/g doxorubicin concentration at the ablation boundary (targeted site of action), the time required was 6 days and 1.5 days for sustained- and dual-release millirods, respectively.

Conclusions. Compared with sustained-release millirods, dual-release millirods provide a quick concentration elevation and sustaining of the drug concentration at the ablation boundary. Additionally, the steady-state drug concentration agrees well with model predictions based on previously determined transport parameters, which demonstrates the feasibility of rational design of drug formulations in polymer millirods.

KEY WORDS: dual-release kinetics; doxorubicin; intratumoral drug delivery; poly(D,L-lactide-*co*-glycolide); radiofrequency ablation.

INTRODUCTION

In cancer chemotherapy, it has been a major challenge to maintain the drug concentration within the therapeutic window at the desired sites of action. The disadvantage of intermittent intravenous (IV) administration is that the plasma drug concentration varies periodically. High plasma concentrations of drugs lead to toxicity and patient morbidity whereas low drug concentrations cause insufficient therapeutic effects and sometimes drug resistance (1–3). In the past, the only means of achieving constant drug plasma concentration was through continuous IV infusion of a drug to compensate drug clearance (4–8). However, this procedure requires constant monitoring of plasma concentrations by physicians in a hospital. Moreover, the plasma concentrations do not necessarily reflect the drug concentrations in tumors. In fact, due to the many physiological barriers (e.g., high interstitial pressure in tumors), the drug delivery efficiency to tumors is quite low in systemic chemotherapy (9,10).

To circumvent these limitations, implantable intratumoral drug delivery systems provide alternative means for a safe, efficient, and convenient chemotherapy. The delivery systems are implanted inside the solid tumors for local chemotherapy (11–15). Sustained-release kinetics is the conventional practice and the preferred design in most of the systems. Sustained drug concentration within the therapeutic window increases the possibility of cell killings (16–19).

Currently, our lab is developing a millirod therapy for intratumoral delivery of anticancer drugs into liver tumors treated with radiofrequency (rf) ablation (20–23). rf ablation is a widely used, minimally invasive technique that destroys the majority of tumor tissue by heat. It has been reported, however, that a small portion of cancer cells can survive rf ablation at the ablation boundary, which leads to tumor recurrence (24–27). To prevent tumor recurrence, we will implant polymer millirods into the ablated region for controlled release of an anticancer drug, doxorubicin, to eliminate the residual cancer cells. In the millirod therapy, a transport process and a time period are required before the drug reaches the site of action (ablation boundary).

Most human cancer cells have a short doubling time that ranges from 12 to 48 h (28,29). We hypothesize that polymer millirods that not only provide a sustained drug concentration level at the ablation boundary, but also reach this level quickly after implantation can most effectively prevent tumor escalation and/or metastasis. Figure 1 illustrates our targeted drug concentration–time curve at the ablation boundary, where t_1 is the time needed to reach the therapeutic concentration, and t_2 is the time of drug concentration within the therapeutic window. Our millirod therapy aims to shorten the t_1 and prolong the t_2.

To achieve this pharmacokinetic profile at the ablation boundary, we conceptualized the design of polymer millirods with dual-release kinetics, an initial burst release followed by a sustained-release of drugs (20). In addition, we established a mathematical model, which is based on drug transport from millirod-tissue interface into ablated and nonablated liver tissues, to provide a quantitative design of burst dosage and sustained-release rates. Previous work has shown the feasibility of fabrication of dual-release millirods and independent control of burst doses and sustained-release rates *in vitro* (20). Recently, we also determined the key parameters governing doxorubicin transport in rf-ablated liver tissues from burst-release millirods (30). Potentially, these parameters and the mathematical model will allow the prediction of drug concentration at the ablation boundary and permit the quantitative design of dose formulations in dual-release millirods.

In order to validate the dual-release design *in vivo*, the current study used rf-ablated rat livers to compare and evaluate the local doxorubicin pharmacokinetics from sustained- and dual-release millirods. The experimental results were also compared to the model predictions to validate the model design in the millirod development.

[1] Department of Biomedical Engineering, Case Western Reserve University, Cleveland, Ohio 44106.

[2] Department of Surgery, Case Western Reserve University School of Medicine, Cleveland, Ohio 44106.

[3] To whom correspondence should be addressed. (e-mail: jinming@cwru.edu)

[4] Current address: Exploratory Biopharmaceutics and Stability, Bristol-Myers Squibb Company, One Squibb Drive, P.O. Box 191, New Brunswick, NJ 08903.

0724-8741/04/0300-0394/0 © 2004 Plenum Publishing Corporation

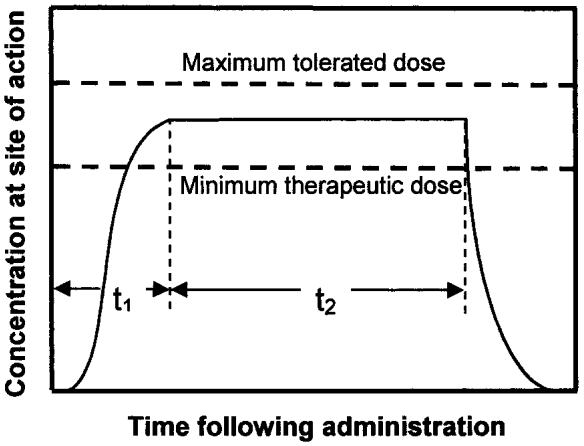

Fig. 1. Targeted drug concentration–time relationship at the site of action (ablation boundary). t_1: time needed for drug concentration to reach therapeutic level. t_2: time that the drug concentration is maintained within the therapeutic window.

MATERIALS AND METHODS

Animals

Male Sprague Dawley rats (350-450 g) were obtained from the Charles River Laboratories (Boston, MA, USA). Animal procedures adhered to the NIH guidelines and an approved protocol by the Institutional Animal Care and Use Committee (IACUC) at Case Western Reserve University.

Materials

Poly(D,L-lactide) (PLA; inherent viscosity 0.67 dl/g) and poly(D,L-lactide-*co*-glycolide) (PLGA; lactide:glycolide = 1:1, MW 50,000 Da, inherent viscosity 0.65 dl/g) were purchased from Birmingham Polymers, Inc. (Birmingham, AL, USA). Poly(ethylene glycol) (PEG; M_n 4600) and poly(ethylene oxide) (PEO; M_V 200,000) were obtained from Aldrich (Milwaukee, WI, USA). Doxorubicin HCl solution was purchased from Bedford Laboratories (Bedford, OH, USA). Tris-buffered saline solution (1X) was purchased from Fisher Scientific (Pittsburgh, PA, USA).

Development of Sustained- and Dual-Release Millirods

The fabrication of sustained- and dual-release millirods has previously been reported (20,21). Briefly, the doxorubicin HCl solution was desalted by dialysis in distilled water. The purified doxorubicin solution was lyophilized to provide a fine powder. PLGA microspheres (average diameter is 4 μm based on SEM analysis of 50 particles) were produced by a single emulsion procedure (23). Monolithic PLGA millirods containing 5% doxorubicin, 25% NaCl, and 70% PLGA were fabricated by a compression-heat molding procedure (23). The monolithic, cylindrical millirods (1.6 mm in diameter) were cut to 8 mm in length and were used as the inner core for the sustained- and dual-release millirods.

Sustained-release millirods were fabricated by dipping the monolithic PLGA millirods into PEG–PLA solution in CH_2Cl_2 at room temperature. The total polymer concentration was 200 mg/ml and PEG in PLA percentage was 10%. The dipping speed was controlled by a vertically placed syringe pump at 2 mm/s. The millirods were suspended in the fume hood by clamps and air-dried at room temperature for 24 h. The other end was dip-coated and dried with the same procedure. The drug loading density was 1.41 mg/cm for the sustained millirods. The dual-release millirods were formed by further dipping the sustained-release millirods into doxorubicin/PEO suspension (100 mg/ml, 75% doxorubicin, 25% PEO in CH_2Cl_2) with the same procedure. The dip-coating was performed twice for each end of the millirods to form the doxorubicin/PEO layer on the surface of the millirods, with a 24-h air-drying period separating each dipping. The total drug loading density in dual-release millirods is 1.95 mg/cm with 0.63 mg/cm in the burst dose and 1.32 mg/cm in the sustained dose.

Radiofrequency Ablation and Millirods Implantation

Male Sprague Dawley rats were anesthetized with an intraperitoneal injection of sodium pentobarbital (50 mg/kg). The abdomen was shaved and prepared with Betadine and alcohol. A local anesthetic, Marcaine, was injected subcutaneously just prior to the skin incision. The medial lobe of the liver was exposed through a small midline incision and exteriorized for rf thermo-ablation and millirod placement. Tissue ablation was produced using rf-generated current (0.09–0.12 A) from a 19-gauge needle electrode (Radionics, Burlington, MA, USA) at 90 ± 2°C for 2 min. The ablated region extended approximately 4–5 mm from the electrode source. After the electrode was removed, a millirod was placed in the electrode tract, and a small piece of cotton was sewn at the top. At different time points, the animals were sacrificed, and polymer millirods were retrieved for the measurement of retaining doxorubicin. The liver was recovered and sectioned to measure the tissue distribution of doxorubicin.

In vivo Doxorubicin Release

Each polymer millirod retrieved from liver tissue was dissolved completely in 2 ml of *N,N*-dimethylformamide. The solution was diluted 10 times in 1X Tris buffer and centrifuged to precipitate the PLGA polymer. The supernatant was analyzed by UV-Vis spectrophotometer (Perkin-Elmer Lambda 20 model, Boston, MA, USA) at 480 nm to obtain the amount of doxorubicin that remained inside the millirods. The cumulative release of doxorubicin was obtained by subtracting the remaining doxorubicin from the total amount that was loaded in the PLGA millirods (n = 3) and plotting the data over time. The average release rates were calculated by dividing the released amount of doxorubicin in different time periods over the number of hours. The sampling times after millirod implantation were 4 h (dual-release millirods only) and 1, 2, 4, 6, and 8 days.

Doxorubicin Concentration Distribution in Liver Tissues

Doxorubicin concentration in rat livers was analyzed by fluorescence imaging as reported previously (22). Briefly, each liver tissue sample was mounted on a cryostat microtome with O.C.T. embedding medium (Miles Inc., Elkhart, IN, USA) and cut into 100-μm slices. All slices were cut perpendicularly to the millirod long axis. The liver slices were scanned by a fluorescence imager (FluoroImager SI model, Molecular Dynamics, Inc., Sunnyvale, CA, USA), and the

fluorescence images were saved in TIFF format with 2^{16} gray level. Fluorescence intensity in the images was converted to drug concentration by MatLab software (version 5.3) based on a predetermined calibration curve (22). Image J software (free from NIH) was used to calculate the doxorubicin concentrations in ablated tissues at the millirod interface and radially outward. The concentration–distance profile in one animal was averaged from six radial directions, approximately 60° between each direction. The average profile at any time point was obtained from three animals.

RESULTS

In vivo Doxorubicin Release Kinetics from Sustained- and Dual-Release Millirods

Sustained- and dual-release millirods were implanted in rat livers after rf ablation, and their release kinetics were characterized over 8 days. As described previously (20), sustained-release millirods provide a prolonged release of drugs via the semipermeable PEG–PLA layer, and the release rates can be controlled by the percentage of PEG in the PLA phase. In comparison, dual-release millirods achieve the initial burst release through the quick dissolution of water-soluble PEO–doxorubicin layer followed by sustained release through the PEG–PLA membrane-encased monolithic millirods (20). In this study, we used the same sustained-release millirods for the fabrication of the dual-release millirods. Therefore, the dual-release millirods will have the same sustained-release kinetics as the sustained-release millirods in addition to the burst dose from the PEO–doxorubicin layer.

Figure 2A compares the cumulative doxorubicin release profiles from sustained- and dual-release PLGA millirods in ablated livers. For the sustained-release millirods, the total drug-loading density was 1.41 mg/cm. After 24 h, data showed that 0.61 ± 0.08 mg/cm (n = 3) of doxorubicin was released from the sustained millirods, corresponding to 43% of the total dosage. In addition, a majority of the drug (>90%) was released from the sustained millirods 144 h (6 days) after implantation. In comparison, dual-release millirods released 0.63 ± 0.12 mg/cm (n = 3) of doxorubicin only after 4 h, which is consistent with the burst dose design in the dual-release millirods. After 24 h, 1.14 ± 0.15 mg/cm (n = 3) of doxorubicin was released from the dual-release millirods, almost twice as much as that (0.61 ± 0.08 mg/cm) from the sustained millirods at the same time. After 192 h (8 days), almost all the drug dosage was released from both types of millirods. It should be noted that dual-release millirods have an extra amount of drug loading due to the introduction of the burst dose.

Figure 2B compares the average release rates in different time periods for both types of millirods. Data showed that the average release rate from the dual-release millirods was significantly higher than that from sustained millirods in the initial time periods (0–24 h). More specificly, the average release rates were 45 ± 5 and 26 ± 2 μg/ (cm h) from dual-release and sustained millirods, respectively (p value = 0.005). For the time after 24 h, the average release rates were comparable and statistically insignificant between the dual-release and sustained millirods (Fig. 2B). This is reasonable because the dual-release millirods use the same sustained millirod design for the sustained phase of the drug release.

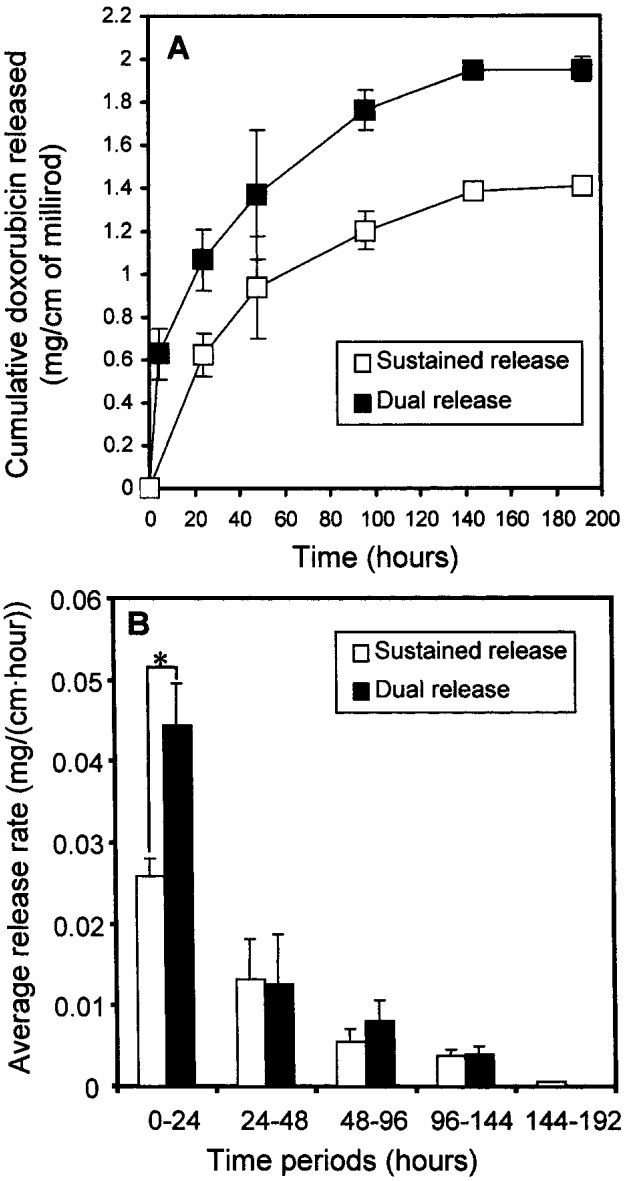

Fig. 2. (A) Cumulative release of doxorubicin from sustained- (□) and dual-release millirods (■) in rf-ablated rat livers *in vivo*. (B) Average doxorubicin release rates from sustained- and dual-release millirods at different time periods *in vivo*. The asterisk shows the average release rates in 0–24 h are statistically significant between sustained- and dual-release millirods (p = 0.005). The error bars were measured from triplicate samples.

Therefore, the major difference between the dual-release and sustained-release millriods is the initial burst release phase introduced by the PEO–doxorubicin layer in the dual-release millirods.

Distribution of Doxorubicin in Ablated Liver Tissues by Fluorescence Imaging

At different time points following millirod implantation, rat livers were removed, frozen, and sectioned to examine the doxorubicin concentration distribution by fluorescence imaging. Figure 3 illustrates the representative liver slices from sustained- and dual-release millirods over 8 days. By gross inspection, 1 day after implantation of sustained-release mil-

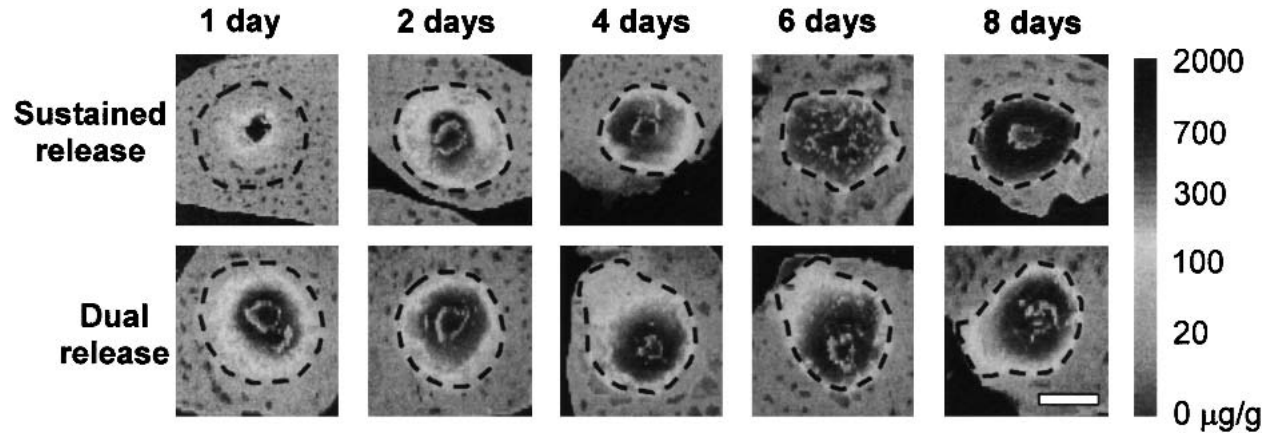

Fig. 3. Comparison of doxorubicin distribution in ablated rat liver tissues after release from sustained- and dual-release millirods. The dashed lines in each image represent the ablation boundary, and the color bar represents the doxorubicin concentration scale in liver tissues. The scale bar is 5 mm.

lirods, doxorubicin was localized around the implantation site, and almost no detectable amount of doxorubicin was observed beyond 2–3 mm into the ablated liver tissue. By day 2, drug reached the ablation boundary while the overall drug concentration inside the ablated region was relatively low. From 4 to 8 days, the radius of the drug distribution region (4–5 mm) became comparable to the radius of the ablated tissue (~4 mm). The overall drug concentration within the ablated region appeared to increase gradually from 2 to 8 days. In contrast, dual-release millirods led to doxorubicin distribution that covered the entire ablated region only 1 day after millirod implantation. The concentration distribution profiles did not change drastically over 8 days. Qualitative examination of the fluorescence intensities inside the ablated region showed that the overall drug concentration in the ablated regions were higher with dual-release millirods than sustained-release millirods in the first 4 days. These results demonstrate the effectiveness of burst dosage in dual-release millirods to elevate quickly the drug concentrations inside ablated tissues following implantation.

Quantitative Comparison of Doxorubicin Pharmacokinetics in Ablated Liver Tissues

Figure 4 compares the local doxorubicin pharmacokinetics at the millirod-tissue interface and ablation boundary between the sustained and dual-release millirods. When sustained millirods were used, there was a 2-day delay before the concentration at the millirod–tissue interface reached 730 ± 106 μg/g, then remaining in the range between 628 ± 146 and 785 ± 77 μg/g over the following 2–8 days (Fig. 4A). In contrast, dual-release millirods boosted doxorubicin concentration at the millirod–tissue interface up to 781 ± 69 μg/g after only 4 h; the concentration further increased up to 1647 ± 232 μg/g after 2 days, then decreased and remained within the range between 925 ± 182 to 1200 ± 82 μg/g within 4–8 days after millirod implantation.

At the ablation boundary (Fig. 4B), doxorubicin concentration increased gradually over the 8-day period after implantation of sustained-release millirods. There was no detectable concentration at the boundary after 1 day. The concentration increased to 8.6 ± 1.4 μg/g at day 2, 12.3 ± 1.0 μg/g at day 4, 25.8 ± 4.5 μg/g at day 6, and 27.5 ± 4.6 μg/g at day 8. In contrast, concentration at the ablation boundary increased rapidly after dual-release millirods were implanted. The concentration increased to 10.3 ± 0.4 μg/g 1 day after implantation and remained between 31.8 ± 2.6 and 43.7 ± 4.4 μg/g during 2–8 days. To achieve comparable doxorubicin concentration of 30–40 μg/g at the ablation boundary, it took 6–8 days for sustained-release millirods but only 1–2 days for dual-release millirods.

DISCUSSION

Comparison of Experimental Data with Model Design

To achieve the drug concentration–time profile with "short t_1 and prolonged t_2" at the ablation boundary (targeted site of action), the burst dose and the sustained release rate of a dual-release millirod can be appropriately designed based on the size of the ablated region, the targeted drug concentration at the ablation boundary, and the quantitative drug transport characteristics in the tissue environment.

We have previously established a mathematical model that describes the drug transport from the millirod-tissue interface into ablated and nonablated liver tissues (20,30). This model took into consideration the transport processes such as drug diffusion, tissue binding, and drug clearance in ablated and nonablated tissues. For a millirod with constant release rate of drug, the steady-state drug concentration C_s at the ablation boundary is

$$C_s = \frac{(r_p/r_s)(J/\beta D_n^*)K_0(\beta r_s)}{K_1(\beta r_s)} \quad (1)$$

where r_p and r_s are the radii of polymer millirod and ablated region, respectively, J is the drug release flux, $K_0(\beta r)$ is the modified Bessel function of zero order, $K_1(\beta r)$ is the modified Bessel function of the first order, and

$$\beta = \sqrt{\frac{\gamma^*}{D_n^*}}.$$

The apparent diffusivities D_a^*, D_n^*, and apparent drug elimination coefficient γ^* are combination parameters that take into consideration doxorubicin–tissue binding. Their physical meanings were previously discussed in detail (30).

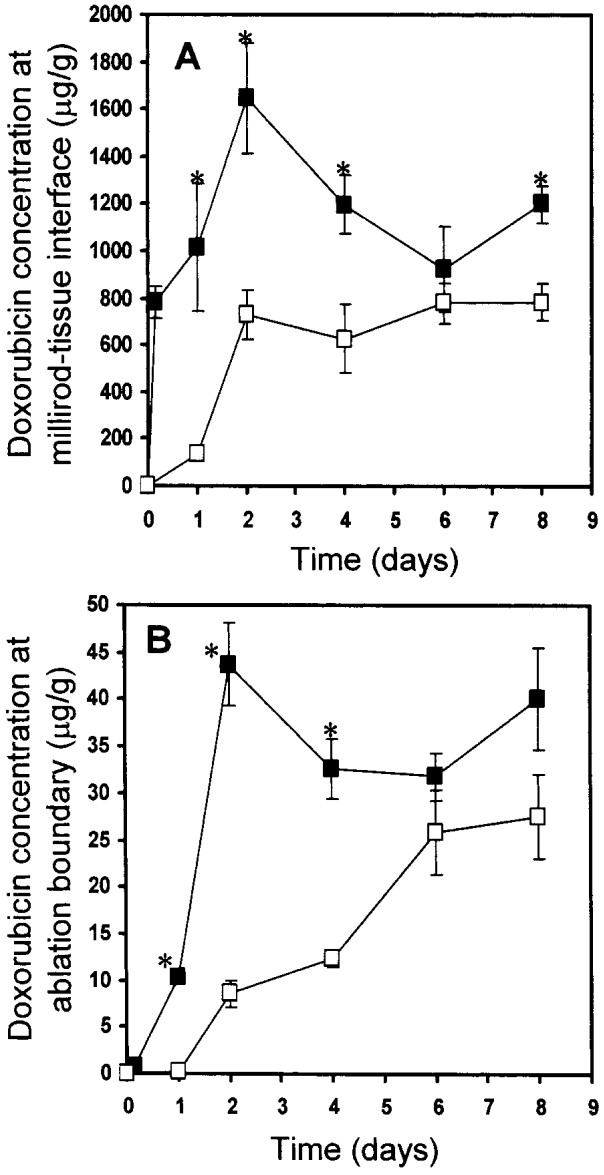

Fig. 4. Doxorubicin concentration–time curves in ablated rat liver tissues at (A) millirod-tissue interface and (B) ablation boundary after implantation of sustained- (□) and dual-release (■) millirods. The data labeled with asterisks are statistically significant ($p < 0.01$, $n = 6$) between the sustained- and dual-release millirods at different time points.

For the model design, the burst dose (A_B) of the dual-release millirods was approximated as the amount of drug inside the ablated region at the steady state:

$$A_B = \frac{R_D}{4D_a^*}\left[2r_p^2 \ln\left(\frac{r_p}{r_s}\right) + r_s^2 - r_p^2\right] + \frac{C_T(r_s^2 - r_p^2)}{2r_p} + \frac{R_D}{D_n^*} \quad (2)$$

R_D is the drug release rate per unit length of millirod and is proportional to the drug flux:

$$R_D = 2\pi r_p J = 2\pi\beta D_n^* r_s C_s K_1(\beta r_s)/K_0(\beta r_s) \quad (3)$$

Recently, we estimated the model transport parameters with a nonlinear least squares method (30). The apparent diffusivities of doxorubicin in ablated and nonablated liver tissue are estimated to be 1.1×10^{-7} cm^2 s^{-1} and 6.7×10^{-7} cm^2 s^{-1}, respectively; the apparent doxorubicin elimination coefficient in nonablated tissue was estimated as 9.6×10^{-4} s^{-1}. Using Eq. (1), we predicted the steady-state drug concentration at the ablation boundary from the polymer millirods.

The overall average release rate of the sustained-release millirods over 8 days was 7.29×10^{-3} mg/(cm h), and the overall average release rate of the dual-release millirods from 4 h to 8 days was 7.02×10^{-3} mg/(cm h). According to the model prediction, the steady-state drug concentrations at the ablation boundary were 30.7 and 29.6 μg/g for sustained-release and dual-release millirods, respectively. The experimental data (Fig. 4B) showed that the drug concentrations at the ablation boundary reached relatively stable ranges using both types of millirods. For sustained-release millirods, the boundary concentrations reached the value of 25.8 ± 4.5 μg/g at 6 days and 27.5 ± 4.6 μg/g at 8 days; for dual-release millirods, it reached 43.7 ± 4.4 μg/g at 2 days and 31.8 ± 2.6 μg/g at 8 days. These values are consistent with the model predictions. Vice versa, these data also demonstrate the feasibility of using mathematical models to predict the necessary sustained drug release rate to target a specific drug concentration at the ablation boundary.

In the previous model design, the burst dose (A_B) was approximated by integrating the steady-state concentration distribution over both the ablated and nonablated regions (30). To target a boundary concentration of 30 μg/g, the burst dose was predicted to be 3.6 mg/cm. In the current study, the dual-release millirods contained a burst dose of 0.63 mg/cm; only 17.5% of the predicted value. Experimental data showed that this burst dose still significantly shortened the t_1 (Fig. 4B), which suggests a smaller value of A_B may be sufficient to elevate the drug concentrations inside ablated tissue. For a more accurate estimation of burst dose, the dynamic model equations must be solved with a specified time-varying release rate. Future *in vivo* studies with millirods of different burst doses are necessary to optimize and validate the rational design of burst dose.

The Pharmacokinetic Advantage of Dual-Release Millirods

In systemic chemotherapy, introduction of a burst dose followed by continuous infusion of drugs has clinically been used to provide an immediate therapeutic effect as well as maintaining the plasma drug concentration within the therapeutic window over time (31). In the current study, we applied this pharmacokinetic concept toward the design of our millirods for the *local* delivery of anticancer drugs. We hypothesize that polymer millirods that quickly deliver drugs at cytotoxic concentrations to the ablation boundary and maintain the concentration level for a prolonged time period have the best chance to prevent tumor recurrence following rf ablation (Fig. 1).

The concept of sustained release (prolonged t_2) has been well accepted and implemented in a variety of drug delivery systems, including the current design. After certain time period, sustained drug release from either sustained- or dual-release millirods (later phase) can achieve a relatively stable drug concentration at the ablation boundary. In our application, however, it is essential to introduce the initial burst release to provide a rapid drug elevation at the ablation boundary (short t_1). The experimental results clearly show that dual-

release millirods have obvious advantages in shortening t_1 compared with sustained millirods (Fig. 3 and Fig. 4B). More specifically, dual-release millirods delivered doxorubicin 4–5 days earlier than the sustained ones to the ablation boundary with comparable concentration (Fig. 4B). Because of the short doubling time of cancer cells (12–48 h) and the possibility of tumor metastases, the initial burst may be critical to provide an immediate drug treatment of the ablated tumors. In addition, studies have shown that the extent of cell killings achieved with the first drug exposure can be crucial for the success of chemotherapy, and continuous administration of a low concentration of anticancer drugs can cause drug resistance instead of the desired therapeutic effect (1–3). Results from this study demonstrate that dual-release millirods achieved the desired local drug pharmacokinetics in the ablated tissue. Current work is in progress to validate the therapeutic efficacy of the dual-release millirods in treating rabbit VX-2 liver tumors following rf ablation.

CONCLUSIONS

As an initial validation of our dual-release design *in vivo*, this work successfully demonstrated the pharmacokinetic advantages of dual-release millirods in providing a favorable concentration–time relationship at the ablation boundary over sustained-release millirods. In addition, experimental data verified the usefulness of mathematical models in predicting the drug concentration at the site of action (ablation boundary). Results from this study established the pharmacokinetic principles of dual-release design for future tumor efficacy studies.

ACKNOWLEDGMENT

This work was supported by the National Institutes of Health (R01-CA-90696).

REFERENCES

1. A. Berman, L. Chisholm, M. de Carvalho, J. A. Piemme, and C. R. Gorrell. Cancer chemotherapy: intravenous administration. *Cancer Nurs.* **16**:145–158 (1993).
2. G. Ganem, P. Carde, and A. Gouyette. Prolonged intravenous infusion chemotherapy. General review of theoretical bases and results. *Bull. Cancer* **72**:491–505 (1985).
3. E. M. Copeland III. Intravenous hyperalimentation and chemotherapy: an update. *JPEN J. Parenter. Enteral Nutr.* **6**:236–239 (1982).
4. J. Lokichand and N. Anderson. Dose intensity for bolus versus infusion chemotherapy administration: review of the literature for 27 anti-neoplastic agents. *Ann. Oncol.* **8**:15–25 (1997).
5. M. C. Sheen. Arterial infusion chemotherapy in far advanced cancer. *Gan To Kagaku Ryoho* **21**:2089–2100 (1994).
6. Y. Arai, C. Kido, and Y. Ariyoshi. Pharmacokinetics in arterial infusion chemotherapy. *Gan To Kagaku Ryoho* **20**:1755–1761 (1993).
7. J. Greidanus, P. H. Willemse, D. R. Uges, E. T. Oremus, Z. J. De Langen, and E. G. De Vries. Continuous infusion of low-dose doxorubicin, epirubicin and mitoxantrone in cancer chemotherapy: a review. *Pharmaceutisch Weekblad. Scientific Edition (Utrecht).* **10**:237–245 (1988).
8. R. W. Carlson and B. I. Sikic. Continuous infusion or bolus injection in cancer chemotherapy. *Ann. Intern. Med.* **99**:823–833 (1983).
9. R. K. Jain. Delivery of molecular and cellular medicine to solid tumors. *Adv. Drug Deliv. Rev.* **46**:149–168 (2001).
10. R. K. Jain. Vascular and interstitial barriers to delivery of therapeutic agents in tumors. *Cancer Metastasis Rev.* **9**:253–266 (1990).
11. H. Brem and R. Langer. Polymer-based drug delivery to the brain. *Science and Medicine* **3**:52–61 (1996).
12. A. K. Dash and G. C. Cudworth II. Therapeutic applications of implantable drug delivery systems. *J. Pharmacol. Toxicol. Methods* **40**:1–12 (1998).
13. W. M. Saltzman and L. K. Fung. Polymeric implants for cancer chemotherapy. *Adv. Drug Deliv. Rev.* **26**:209–230 (1997).
14. M. Kurisawa and N. Yui. Recent trends in drug delivery systems using biomaterials. *Nippon Rinsho* **54**:2004–2011 (1996).
15. A. Oliviand and H. Brem. Interstitial chemotherapy with sustained-release polymer systems for the treatment of malignant gliomas. *Recent Results Cancer Res.* **135**:149–154 (1994).
16. G. I. Shapiro and J. W. Harper. Anticancer drug targets: cell cycle and checkpoint control. *J. Clin. Invest.* **104**:1645–1653 (1999).
17. M. J. Egorin. Overview of recent topics in clinical pharmacology of anticancer agents. *Cancer Chemother. Pharmacol.* **42**:S22–S30 (1998).
18. I. F. Tannock. Experimental chemotherapy and concepts related to the cell cycle. *Int. J. Radiat. Biol. Relat. Stud. Phys. Chem. Med.* **49**:335–355 (1986).
19. L. M. van Putten. Cell cycle specificity of anticancer agents. *Antibiot. Chemother.* **23**:128–134 (1978).
20. F. Qian, G. M. Saidel, D. M. Sutton, A. Exner, and J. Gao. Combined modeling and experimental approach for the development of dual-release polymer millirods. *J. Controlled Rel.* **83**:427–435 (2002).
21. F. Qian and N. Nasongkla, and J. Gao. Membrane-encased polymer millirods for sustained release of 5-fluorouracil. *J. Biomed. Mater. Res.* **61**:203–211 (2002).
22. J. Gao, F. Qian, A. Szymanski-Exner, N. Stowe, and J. Haaga. In vivo drug distribution dynamics in thermoablated and normal rabbit livers from biodegradable polymers. *J. Biomed. Mater. Res.* **62**:308–314 (2002).
23. F. Qian, A. Szymanski, and J. Gao. Fabrication and characterization of controlled release poly(D,L-lactide-co-glycolide) millirods. *J. Biomed. Mater. Res.* **55**:512–522 (2001).
24. G. D. Dodd III, M. C. Soulen, R. A. Kane, T. Livraghi, W. R. Lees, Y. Yamashita, A. R. Gillams, O. I. Karahan, and H. Rhim. Minimally invasive treatment of malignant hepatic tumors: at the threshold of a major breakthrough. *Radiographics* **20**:9–27 (2000).
25. G. Francica and G. Marone. Ultrasound-guided percutaneous treatment of hepatocellular carcinoma by radiofrequency hyperthermia with a 'cooled-tip needle.' A preliminary clinical experience. *Eur. J. Ultrasound* **9**:145–153 (1999).
26. R. Lencioni, O. Goletti, N. Armillotta, A. Paolicchi, M. Moretti, D. Cioni, F. Donati, A. Cicorelli, S. Ricci, M. Carrai, P. F. Conte, E. Cavina, and C. Bartoloz. Radio-frequency thermal ablation of liver metastases with a cooled-tip electrode needle: results of a pilot clinical trial. *Eur. Radiol.* **8**:1205–1211 (1998).
27. L. Buscarini and S. Rossi. Technology for radiofrequency thermal ablation of liver tumors. *Semin. Laparosc. Surg.* **4**:96–101 (1997).
28. M. R. Grever, S. A. Schepartz, and B. A. Chabner. The National Cancer Institute: cancer drug discovery and development program. *Semin. Oncol.* **19**:622–638 (1992).
29. M. C. Alley, D. A. Scudiero, A. Monks, M. L. Hursey, M. J. Czerwinski, D. L. Fine, B. J. Abbott, J. G. Mayo, R. H. Shoemaker, and M. R. Boyd. Feasibility of drug screening with panels of human tumor cell lines using a microculture tetrazolium assay. *Cancer Res.* **48**:589–601 (1988).
30. F. Qian, N. Stowe, E. H. Liu, and G. M. Saidel, and J. Gao. Quantification of in vivo doxorubicin transport in thermoablated rat livers. *J. Controlled Rel.* **91**:157–166 (2003).
31. L. Z. Benet, D. L. Kroetz, and L. B. Sheiner. Pharmacokinetics, In J. G. Hardman, L. E. Limbird, P. B. Molinoff, and R. W. Ruddon (eds.), *Goodman and Gilman's The Pharmacological Basis of Therapeutics*, 9th edition, McGraw-Hill, New York, 1996, pp. 3–27.